



## A novel mathematical model considering change of diffusion coefficient for predicting dissolution behavior of acetaminophen from wax matrix dosage form<sup>☆</sup>

Yuta Nitani<sup>1</sup>, Yasuyoshi Agata<sup>1</sup>, Yasunori Iwao, Shigeru Itai<sup>\*</sup>

Department of Pharmaceutical Engineering, School of Pharmaceutical Sciences, University of Shizuoka, 52-1 Yada, Suruga-ku, Shizuoka 422-8526, Japan

### ARTICLE INFO

#### Article history:

Received 2 September 2011

Received in revised form 10 February 2012

Accepted 23 February 2012

Available online 1 March 2012

#### Keywords:

Wax matrix

Mathematical model

Time-dependent diffusivity

AMCE

### ABSTRACT

From wax matrix dosage forms, drug and water-soluble polymer are released into the external solvent over time. As a consequence, the pore volume inside the wax matrix particles is increased and the diffusion coefficient of the drug is altered. In the present study, we attempted to derive a novel empirical mathematical model, namely, a time-dependent diffusivity (TDD) model, that assumes the change in the drug's diffusion coefficient can be used to predict the drug release from spherical wax matrix particles. Wax matrix particles were prepared by using acetaminophen (APAP), a model drug; glyceryl monostearate (GM), a wax base; and aminoalkyl methacrylate copolymer E (AMCE), a functional polymer that dissolves below pH 5.0 and swells over pH 5.0. A three-factor, three-level ( $3^3$ ) Box–Behnken design was used to evaluate the effects of several of the variables in the model formulation, and the release of APAP from wax matrix particles was evaluated by the paddle method at pH 4.0 and pH 6.5. When comparing the goodness of fit to the experimental data between the proposed TDD model and the conventional pure diffusion model, a better correspondence was observed for the TDD model in all cases. Multiple regression analysis revealed that an increase in AMCE loading enhanced the diffusion coefficient with time, and that this increase also had a significant effect on drug release behavior. Furthermore, from the results of the multiple regression analysis, a formulation with desired drug release behavior was found to satisfy the criteria of the bitter taste masking of APAP without lowering the bioavailability. That is to say, the amount of APAP released remains below 15% for 10 min at pH 6.5 and exceeds 90% within 30 min at pH 4.0. The predicted formulation was 15% APAP loading, 8.25% AMCE loading, and 400  $\mu$ m mean particle diameter. When wax matrix dosage forms were prepared accordingly, the predicted drug release behavior agreed well with experimental values at each pH level. Therefore, the proposed model is feasible as a useful tool for predicting drug release behavior, as well as for designing the formulation of wax matrix dosage forms.

© 2012 Elsevier B.V. All rights reserved.

### 1. Introduction

Wax matrix dosage forms constructed by insoluble lipids, a wax base, have attracted attention in the pharmaceutical field because this formulation has a number of advantages: organic solvent-free preparation, non-toxicity, and cost effectiveness (Shiino et al., 2010). To date, various wax matrix dosage forms have been

developed for controlled release, taste masking, or both (Kayumba et al., 2007; Xu et al., 2008).

Generally, drug diffusion within wax matrix particles has been considered to be the rate-controlling step of drug release from wax matrix particles, and many studies have investigated the kinetics of drug release from wax matrix dosage forms on the basis of the Higuchi equation (Higuchi, 1961) or Fick's second law of diffusion (Crank, 1975). Yajima et al. (1996) reported that isokinetic erosion derived from polymer characteristics was the rate-controlling step of drug release, and they derived a mathematical model similar to the cube-root law. However, the applicability of Yajima's model is limited to a narrow set of conditions, such as those in the initial stages of dissolution; for long dissolution times, diffusion becomes the dominant step controlling drug release. Against this background, we recently succeeded in deriving a mathematical model that incorporates diffusion and erosion theory, where a decrease in particle diameter of wax matrix particles over time is assumed to predict the kinetics of drug release from wax matrix

**Abbreviations:** APAP, acetaminophen; GM, glyceryl monostearate; AMCE, aminoalkyl methacrylate copolymer E; TDD, time-dependent diffusivity; SEM, scanning electron microscope; AIC, Akaike's information criterion.

<sup>☆</sup> This study was supported, in part, by a Grant-in-Aid for Scientific Research (C) from the Ministry of Education, Culture, Sports, Science and Technology of Japan (No. 23590047).

\* Corresponding author. Tel.: +81 54 264 5614; fax: +81 54 264 5615.

E-mail address: [s-itai@u-shizuoka-ken.ac.jp](mailto:s-itai@u-shizuoka-ken.ac.jp) (S. Itai).

<sup>1</sup> These authors contributed equally to this work.

particles (Agata et al., 2011). Although this model exhibited good agreement with all experimental values pertaining to APAP release at pH 4.0 and pH 6.5, a concern about the initial conditions of this mathematical model remains; namely, that changes of particle diameter are much less likely to occur in wax matrix particles than is assumed in the model. However, another possibility is that an increase in pore volume inside wax matrix particles, rather than a decrease in particle diameter, is involved in the release of drugs from wax matrix particles. Thus, development of a mathematical model that considers time-dependent diffusivity (TDD) is considered to be worth investigated.

So far, a number of mathematical models that consider time- or position-dependent diffusivity have been investigated. For instance, as TDD models, semi-empirical models that consider an increase in pore volume within a cylindrical wax matrix have been analyzed (Siepmann et al., 2008; Verhoeven et al., 2009). In addition, a semi-empirical model that considers a time-dependent changes of polymer molecular weight within wax matrix particles has also been derived (Raman et al., 2005). Although these models represent realistic drug release kinetics, since experimentally determined pore volumes or the initial concentration distribution within the wax matrix dosage forms must be substituted into the models, experiments to obtain these physicochemical parameters are needed. Because previous models are formulated by numerical methods designed to handle more complex processes, the obtained solutions are approximated values and specific knowledge about the mathematics and programming is necessary. Therefore, a new model is required that is easy to formulate and that can obtain a good fit for a variety of general pharmaceutical formulations.

In the present study, we attempted to derive a novel and versatile empirical mathematical model that considers TDD in wax matrix particles, on the basis of Fick's second law without any additional experiments. Since this model can be solved by an exact analytical method, calculations are straightforward. In addition, the model can provide insight into the drug release mechanism within wax matrix particles. By using a spray congealing technique, wax matrix particles were prepared with acetaminophen (APAP) as a model drug, glyceryl monostearate (GM) as a wax base, and aminoalkyl methacrylate copolymer E (AMCE) as a functional polymer that dissolves below pH 5.0 and swells over pH 5.0. The drug release behavior and the validity of the proposed TDD model were then investigated. Furthermore, we sought to predict the desirable kinetics of drug release from wax matrix particles by using a combination of the TDD model and a Box–Behnken design.

## 2. Theory

If we restrict ourselves to a case where the drug diffusion is radial in a single wax matrix particle, the diffusion equation for a sphere takes the form (Crank, 1975)

$$\frac{\partial c}{\partial t} = \frac{1}{r^2} \left\{ \frac{\partial}{\partial r} \left( D r^2 \frac{\partial c}{\partial r} \right) \right\}, \quad (1)$$

where  $c$  denotes the concentration of a drug as a function of time  $t$  and radius  $r$  within the spherical wax matrix particle. Furthermore,  $D$  is the diffusion coefficient of drug.

If  $D$  can change over time during diffusion, the diffusion equation then becomes

$$\frac{\partial c}{\partial t} = \frac{D(t)}{r^2} \left\{ \frac{\partial}{\partial r} \left( r^2 \frac{\partial c}{\partial r} \right) \right\}. \quad (2)$$

Also, if the function  $T$  is defined as

$$T(t) = \int_0^t D(t) dt, \quad (3)$$

then  $dT/dt = D(t)$ . By the chain rule, Eq. (2) can be rewritten as

$$\frac{\partial c}{\partial T} = \frac{1}{r^2} \frac{\partial}{\partial r} \left( r^2 \frac{\partial c}{\partial r} \right). \quad (4)$$

By setting

$$u = rc, \quad (5)$$

Eq. (4) is transformed into

$$\frac{\partial u}{\partial T} = \frac{\partial^2 u}{\partial r^2}. \quad (6)$$

From the assumption that APAP is uniformly distributed throughout the wax matrix particle at the start of the experiment, the initial condition for Eq. (6) is

$$u|_{t=0} = rc_0. \quad (7)$$

Here,  $c_0$  represents the initial APAP concentration in the system. In addition, the boundary conditions for Eq. (6) follow from the assumption that perfect sink conditions are maintained throughout the experiment:

$$u|_{r=a/2} = 0. \quad (8)$$

Here,  $a$  represents the particle diameter. This initial value problem (Eqs. (6)–(9)) can be solved by Laplace transform or separation of variables, leading to

$$c(r, t) = \frac{-ac_0}{\pi r} \sum_{n=1}^{\infty} \frac{(-1)^n}{n^2} \exp \left( -\frac{4n^2\pi^2}{a^2} T(t) \right) \sin \frac{2n\pi}{a} r. \quad (9)$$

The absolute amount of APAP remaining in the system is given by

$$M = \frac{a^3 c_0}{\pi} \sum_{n=1}^{\infty} \frac{1}{n^2} \exp \left( -\frac{4n^2\pi^2}{a^2} T(t) \right). \quad (10)$$

Here,  $M$  represents the absolute remaining amounts of APAP in the system. For  $m$  wax matrix particles having equal diameter, the total amount of drug within the particles is given by

$$mM = m \frac{a^3 c_0}{\pi} \sum_{n=1}^{\infty} \frac{1}{n^2} \exp \left( -\frac{4n^2\pi^2}{a^2} T(t) \right), \quad (11)$$

and the initial total amount of drug is

$$M_{total} = m \frac{1}{6} \pi a^3 c_0. \quad (12)$$

Therefore, the drug release ratio at time  $t$  is given by

$$R = 1 - \frac{6}{\pi^2} \sum_{n=1}^{\infty} \frac{1}{n^2} \exp \left( -\frac{4n^2\pi^2}{a^2} T(t) \right). \quad (13)$$

In this study, an empirical model that reflects the TDD is established. If rate of change of the diffusion coefficient constantly increase and/or decrease in first order proportion to diffusion coefficient, the empirical model is assumed as the following,

$$\frac{dD}{dt} = K - kD, \quad (14)$$

where  $K$  ( $\mu\text{m}^2 \text{min}^{-2}$ ) is the coefficient associated with the rate of increase of the diffusion coefficient, and  $k$  ( $\text{min}^{-1}$ ) is the coefficient associated with the speed that the diffusion coefficient of the wax matrix particles reaches the maximum ( $K/k$ ). If the diffusion coefficient is equal to zero at the start of the experiment, Eq. (14) can be solved to give

$$D(t) = \frac{K}{k} \{1 - \exp(-kt)\}. \quad (15)$$

**Table 1**

Formulation and physicochemical properties of wax matrix particles in each batch.

Batch	APAP loading (%)	AMCE loading (%)	Collected fraction (μm)	Particle diameter (μm)	Circularity
1	10	0	300–420	341.5 ± 28.4	0.957 ± 0.011
2	10	5	210–300	251.7 ± 25.0	0.944 ± 0.043
3	10	5	420–500	466.9 ± 19.5	0.951 ± 0.007
4	10	10	300–420	363.7 ± 40.7	0.948 ± 0.012
5	20	0	420–500	469.5 ± 13.3	0.958 ± 0.006
6	20	0	210–300	252.4 ± 21.3	0.959 ± 0.007
7	20	10	420–500	472.5 ± 20.6	0.954 ± 0.015
8	20	10	210–300	259.1 ± 20.2	0.962 ± 0.008
9	30	0	300–420	363.0 ± 36.7	0.956 ± 0.006
10	30	5	210–300	251.0 ± 18.1	0.952 ± 0.013
11	30	5	420–500	467.5 ± 15.9	0.946 ± 0.014
12	30	10	300–420	361.1 ± 35.2	0.961 ± 0.008
13–15	20	5	300–420	365.3 ± 36.5	0.963 ± 0.007

Then, Eq. (3) can be written as

$$T(t) = \frac{K}{k} \left[ t + \frac{1}{k} (\exp(-kt) - 1) \right]. \quad (16)$$

Thus, the TDD model that describes the drug release behavior is obtained by substituting Eq. (16) into Eq. (13).

For the purpose of comparison, the conventional pure diffusion model with constant diffusivity proposed by Crank (1975) (Eq. (17)) and the hybrid model which was derived from our previous work (Agata et al., 2011) (Eq. (18)), are stated as follows:

$$R_{\text{diffusion}}(t) = 1 - \frac{6}{\pi^2} \sum_{n=1}^{\infty} \exp \left( -\frac{4n^2\pi^2}{a^2} Dt \right), \quad (17)$$

$$R(t) = 1 - \frac{6(a(t))^2}{\pi^2 a^2} \sum_{n=1}^{\infty} \frac{1}{n^2} \exp \left( -\frac{n^2\pi^2}{(a(t))^2} Dt \right), \quad (18)$$

where  $a(t)$  represents the distance of the eroding front from the center of the wax matrix particle at time  $t$ .

### 3. Materials and methods

#### 3.1. Materials

APAP was kindly provided by Iwaki Pharmaceutical Co. Ltd. (Shizuoka, Japan). AMCE (Eudragit EPO) was purchased from Röhm Degussa (Darmstadt, Germany), and GM was purchased from Taiyo Chemical Industry Co. Ltd. (Saitama, Japan). All the reagents used were of the highest grade available from commercial sources.

#### 3.2. Preparation of wax matrix particles by spray congealing technique

Wax matrix particles were prepared by a spray congealing technique. APAP was dried for 12 h at 60 °C and milled with a vibrating sample mill (TI-300, Heiko seisakusho, Japan). The milled APAP was immediately sieved (100 mesh). The mean particle diameter of milled APAP was found to be approximately 60 μm by an analysis of laser micro sizer (LMS-2000e, Seishin Enterprise Co. Ltd., Tokyo, Japan). GM was melted at 115 ± 5 °C, and AMCE was added into the GM solution. After AMCE was completely dissolved, sieved APAP was added into the GM solution. The mixture was then agitated until APAP was sufficiently dispersed. The APAP dispersion was dropped onto a metal disk rotating at about 1700 rpm from a height of approximately 10 cm. The sprayed APAP dispersion immediately solidified into spherical particles. The prepared particles were incubated for 24 h at 40 ± 0.5 °C, and were stored for more than 1 week at room temperature thereafter. After incubation, the APAP-loaded wax matrix particles were sieved into different fractions, each having a range of particle diameters (210–300, 300–420,

and 420–500 μm). In order to select the spherical particles, the particles were spread onto a glass plate tilted at an angle of less than 10°. Finally, any particles that fell from glass plate were collected.

#### 3.3. Circularity and mean particle diameter

Approximately 40–50 wax matrix particles were spread onto a glass plate, and an image was taken under an optical microscope (×40 magnification). The circularity and mean particle diameter were measured with WinROOF image analysis software (version 5.5, Mitani Co. Ltd., Japan) (Table 1). The equation of circularity is given by

$$\text{Circularity} = \frac{4\pi S}{L^2} \quad (19)$$

where  $S$  denotes the area of a matrix particle and  $L$  denotes the perimeter of the particle.

#### 3.4. Box–Behnken design

To effectively investigate correlations between factors influencing drug release from wax matrix dosage forms and the response variables in a small number of experiments, a three-factor, three-level Box–Behnken design was used. This design is suitable for the exploration of quadratic response surfaces and the construction of a second-order polynomial model. Another advantage of this design is that it does not contain combinations for which all factors are simultaneously at their highest or lowest levels; therefore, Box–Behnken designs are useful in avoiding experiments performed under extreme conditions where unsatisfactory results might occur (Anees and Mansoor, 1996; Ferreira et al., 2007). APAP loading, AMCE loading, and particle diameter were chosen as factors to be investigated in the present study. Correlations between levels and each independent factor are listed in Table 2. Especially, the factor  $x_3$  was based on the results of particle diameters as shown in Table 1.

#### 3.5. Scanning electron microscopy

The surface morphology of the prepared wax matrix particles was assessed by scanning electron microscopy (SEM) (JEOL JSM-5200, Japanese Electron Optics Laboratory Co. Ltd., Tokyo, Japan).

**Table 2**

Variables and their corresponding levels for wax matrix particles.

Level	Factor $x_1$ : APAP loading (%)	Factor $x_2$ : AMCE loading (%)	Factor $x_3$ : particle diameter (μm)
–1	10	0	250
0	20	5	360
1	30	10	470

The classified wax matrix particles were affixed onto specimen stubs with double-sided carbon conductive adhesive strips and vacuum coated with platinum in a sputter coater (JFC-1600, Japanese Electron Optics Laboratory Co. Ltd., Tokyo, Japan). Each deposited specimen was set on a sample holder, and images were taken with an accelerating voltage of 10 kV (magnification  $\times 200$ ).

### 3.6. In vitro drug release studies

The release of APAP from the wax matrix dosage forms was examined by the paddle method listed in the Japanese Pharmacopeia (16th edition). The test solution was 900 mL of either pH 4.0 acetate buffer solution or pH 6.5 phosphate buffer solution, and the solution was heated to  $37.0 \pm 0.5^\circ\text{C}$ . The paddle rotation speed was 50 rpm. Wax matrix particles (500 mg) from each batch were put into the test solutions. Since wax matrix particles of some batches floated during a dissolution test, a part of the dissolution medium was carefully collected by using a pipette, and then put on the floating particles in order to sink the particles into the test solutions. At appropriate time intervals, 5 mL samples of the test solutions were withdrawn and filtered through a membrane filter (0.45  $\mu\text{m}$ ). The amount of APAP released into the medium was quantitatively determined by UV spectroscopy at 243 nm (UV-mini, Shimadzu Co., Kyoto, Japan).

### 3.7. Curve fitting

Eqs. (13), (17) and (18) were fitted to the set of experimentally determined values by a nonlinear least-squares method using the Levenberg–Marquardt algorithm.

### 3.8. Comparison of consistency between experimental data and curve obtained by mathematical models

Akaike's information criterion (AIC) (Neau et al., 1999) was used as a measure of goodness of fit of the experimental data to Eq. (13), (17) or (18). AIC is given by

$$\text{AIC} = N \ln(\text{RSS}) + 2P, \quad (20)$$

where  $N$  is the number of experimental data, RSS is the residual sum of squares, and  $P$  is the number of parameters.

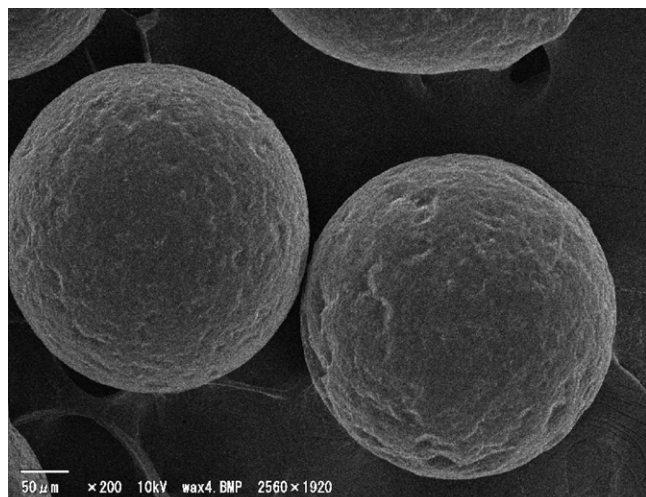


**Fig. 1.** SEM image of wax matrix particles prepared with 30% APAP, 10% AMCE, and 60% GM (batch 12).

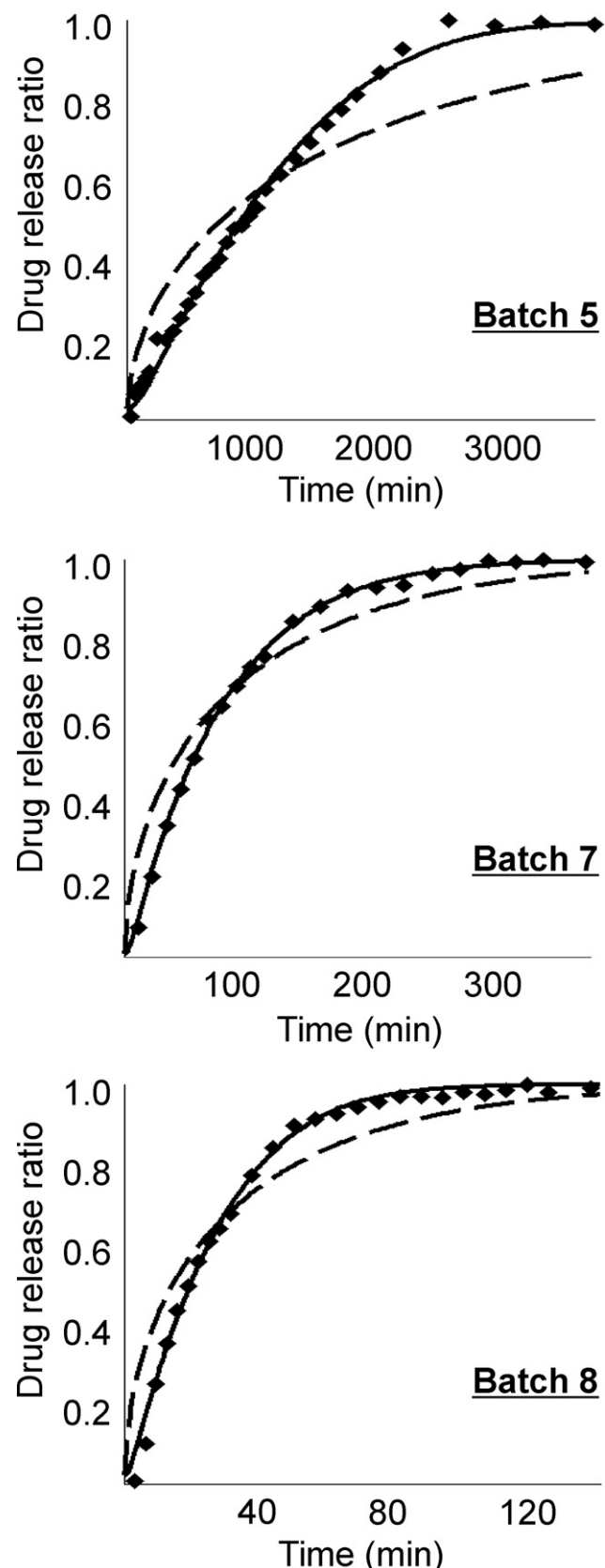


**Fig. 2.** APAP release behavior from wax matrix particles with various formulations (batch 5, 7 and 8) in phosphate buffer at pH 6.5. Symbols: experimental values; solid curves: Eq. (13); and dashed curves: Eq. (17) ( $n = 1$ ).

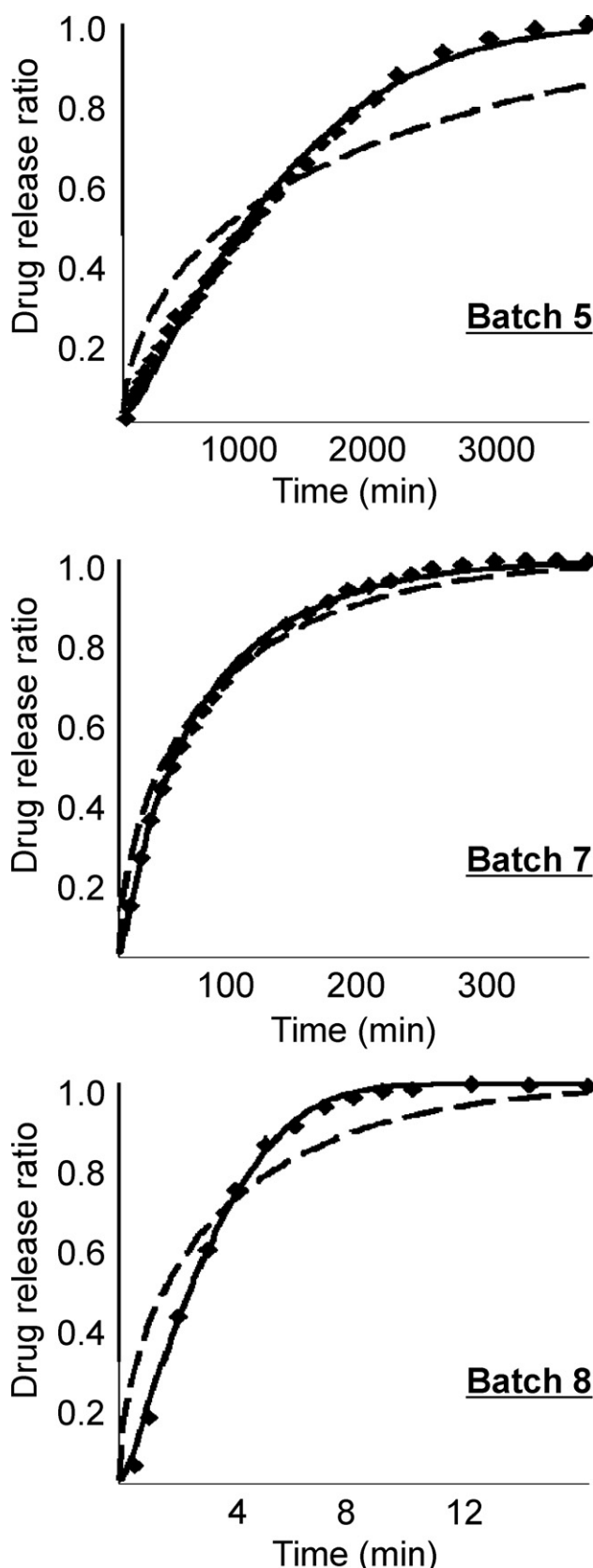


**Fig. 3.** APAP release behavior from wax matrix particles with various formulations (batch 5, 7 and 8) in acetate buffer at pH 4.0. Symbols: experimental values; solid curves: Eq. (13); and dashed curves: Eq. (17) ( $n=1$ ).

### 3.9. Multiple regression analysis

Multi-regression analysis was conducted by using ALCORA (Takayama et al., 1990). The following equation was fitted to each collected parameter,  $x$ , based on the Box–Behnken design, and a response surface was created in order to determine the relationship between each parameter and the drug release behavior,  $Y$ :

$$Y = \sum c_n x_1^i x_2^j x_3^k, \quad (21)$$

where  $c_n$  denotes the partial regression coefficient of the  $n$ th terms.

## 4. Results and discussion

### 4.1. Physicochemical characteristics of the wax matrix dosage forms

Wax matrix particles were prepared by a spray congealing technique, which is gaining considerable attention from the viewpoints of safety and of rapidity in particular. The spray congealing technique for atomizing a solution which contains a drug into a molten carrier overcomes the problem of having residual solvents, and the atomized droplets quickly solidify, owing to their exposure to

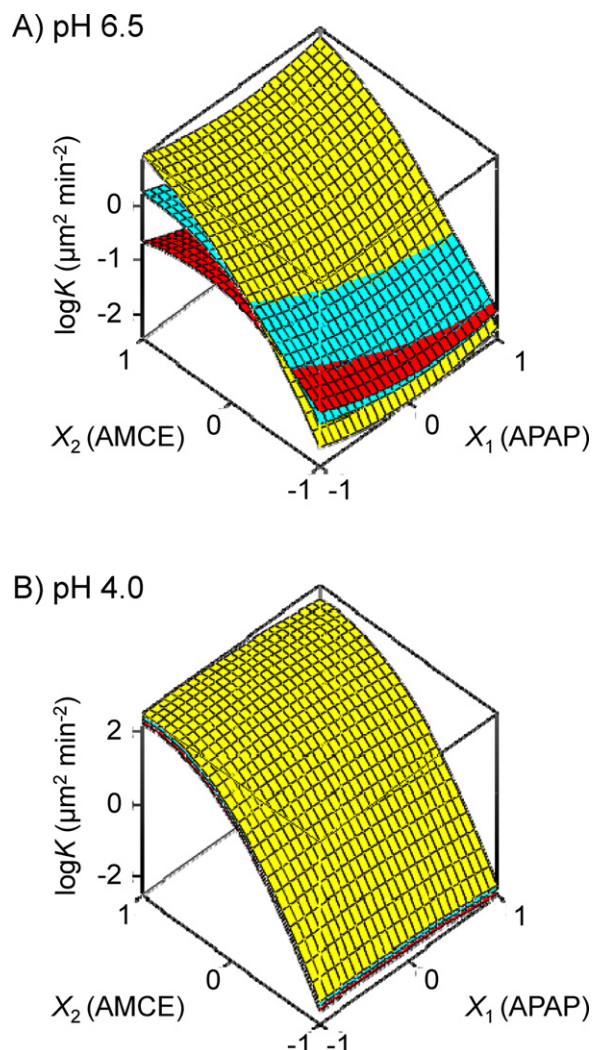


**Fig. 4.** Response surfaces of coefficient  $\log K$  for  $x_1$ ,  $x_2$ , and  $x_3$  at (A) pH 6.5 and (B) pH 4.0. Red,  $x_3 = 1$ ; blue,  $x_3 = 0$ ; and yellow,  $x_3 = -1$ . (For interpretation of the references to color in this figure legend, the reader is referred to the web version of the article.)

**Table 3**

Estimated AIC values for the TDD model, conventional pure diffusion model and hybrid model for each batch at pH 6.5 and pH 4.0.

Batch	pH 6.5			pH 4.0		
	TDD	Conventional	Hybrid	TDD	Conventional	Hybrid
1	-136	-59.8	-141	-136	-48.5	-118
2	-112	-84.1	-101	-109	-72.2	-85.2
3	-160	-98.1	-191	-101	-63.5	-93.1
4	-162	-61.7	-130	-137	-65.5	-95.2
5	-205	-31.4	-151	-126	-35.9	-79.6
6	-193	-45.9	-107	-75.3	-46.2	-100
7	-189	-56.1	-101	-156	-85.0	-144
8	-104	-36.1	-78.6	-73.0	-34.2	-27.2
9	-157	-29.5	-126	-152	-33.4	-65.5
10	-117	-81.9	-145	-90.0	-38.5	-74.0
11	-183	-52.3	-204	-109	-45.2	-99.8
12	-216	-45.6	-133	-146	-46.6	-94.6
13	-147	-66.7	-135	-109	-59.5	-108
14	-155	-75.0	-139	-136	-68.8	-104
15	-152	-70.0	-151	-120	-67.7	-111

ambient air flow (Albertini et al., 2008). Fig. 1 shows SEM image of wax matrix particles containing 30% APAP and 10% AMCE (batch 12) and the wax matrix particles were found to be spherical with a smooth surface, suggesting that the prepared wax matrix particles can be considered true spheres. For all other prepared batches, similar morphologies for the wax matrix particles were also observed (data not shown).

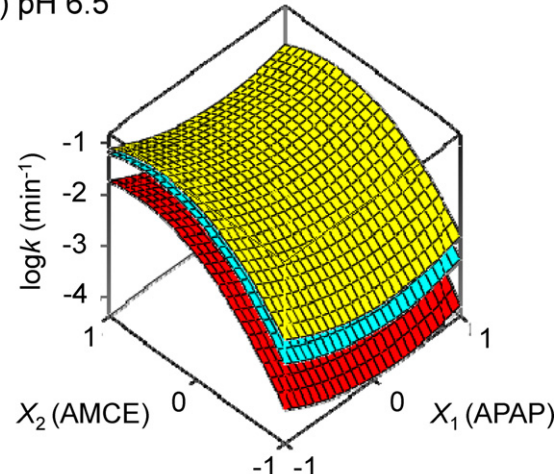
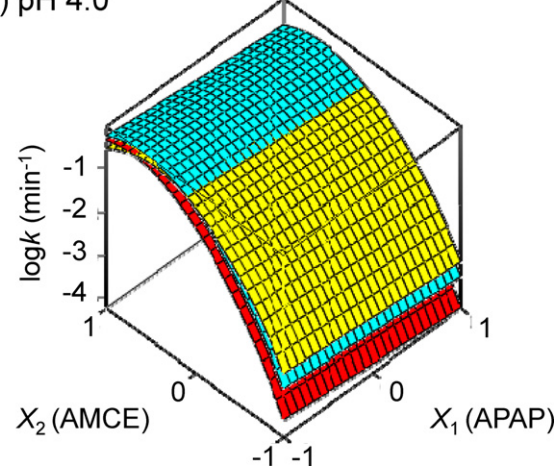
Table 1 shows the circularity of wax matrix particles from the various formulations. The circularity of the particles was over 0.94 for all formulations. From the results shown in Fig. 1 and Table 1, the application of Eqs. (13) and (17) to the obtained wax matrix particles is valid, since the premise of both equations is that the wax matrix particles are spherical.

#### 4.2. Drug release behavior of APAP from wax matrix particles and curve fitting

Figs. 2 and 3 show APAP release behavior from wax matrix dosage forms such as batch 5, 7 and 8 in phosphate buffer at pH 6.5 and acetic buffer at pH 4.0, respectively. The symbols represent the experimental results, and the solid and dashed curves represent the results of fitting Eqs. (13) and (17) to the data, respectively. In all cases, agreement with the experimental values was better for the TDD model (Eq. (13)) than for the pure diffusion model (Eq. (17)) across each time range. For all other prepared batches, similar results were also observed (data not shown). In the fitting results for Eq. (17), at the early stage of dissolution, diffusional mass transport was theoretically overestimated, whereas at latter stages of dissolution, it was underestimated (Fig. 2, dashed curves). This change in the estimation suggested that the diffusion coefficient gradually increased over time, owing to an increase in the pore volume within the wax matrix particles. To quantitatively compare the goodness of fit of each model, AIC values were calculated for each case (Table 3). At both pH levels, all AIC values for the TDD model are smaller than those for the pure diffusion model, suggesting that a

better fit to the experimental data was achieved by the TDD model. The results indicated that drug release behavior was not controlled by only pure diffusion and that the TDD model, which considers time-dependent diffusivity, might be closer to the reality of the situation.

Recently, we succeeded in deriving an empirical mathematical model (hybrid model), based on diffusion and erosion theory, that assumes a decrease in the particle diameter of wax matrix particles over time; good agreement between the theory and experimental values was obtained (Agata et al., 2011) similar to the TDD model presented here. However, changes in the particle diameter of the wax matrix particles were rarely found to occur; namely, when measuring the mean particle diameters of wax matrix particles in batch 1, 6 and 9 before and after drug release study, no significant changes of the particle diameter were observed (Table 4). Hence, application of our previous model to the current formulation might be considered undesirable. In fact, when quantitatively comparing the goodness of fit of hybrid model with that of TDD model, almost all AIC values for the TDD model are also smaller than those for the hybrid model (Table 3), suggesting that a better fit to the experimental data was achieved by the TDD. Mönkäre et al. (2010), however, reported that a reduction of particle size in a wax matrix formulation containing poly

**A) pH 6.5****B) pH 4.0**

**Fig. 5.** Response surfaces of coefficient  $\log k$  for  $x_1$ ,  $x_2$ , and  $x_3$  at (A) pH 6.5 and (B) pH 4.0. Red,  $x_3 = 1$ ; blue,  $x_3 = 0$ ; and yellow,  $x_3 = -1$ . (For interpretation of the references to color in this figure legend, the reader is referred to the web version of the article.)

**Table 4**

Mean particle diameters of wax matrix particles before and after drug release study in 1, 6, and 9 batches.

Batch	Particle diameter ( $\mu\text{m}$ ) Before dissolution	Particle diameter ( $\mu\text{m}$ ) After dissolution
1	$341.5 \pm 28.4$	$354.6 \pm 29.4$
6	$252.4 \pm 21.3$	$259.0 \pm 20.4$
9	$363.0 \pm 36.7$	$337.2 \pm 43.8$

**Table 5**Estimated values of  $K$  and  $k$  for each batch at pH 6.5 and pH 4.0.

Batch	$K$ ( $\mu\text{m}^2 \text{min}^{-2}$ )		$k$ ( $\text{min}^{-1}$ )	
	pH 6.5	pH 4.0	pH 6.5	pH 4.0
1	$2.13 \times 10^{-2}$	$1.03 \times 10^{-2}$	$3.66 \times 10^{-3}$	$1.46 \times 10^{-3}$
2	$8.56 \times 10^{-1}$	$7.16 \times 10$	$4.66 \times 10^{-2}$	$5.41 \times 10^{-1}$
3	$3.31 \times 10^{-1}$	$2.23 \times 10$	$1.93 \times 10^{-2}$	$1.57 \times 10^{-1}$
4	1.60	$1.15 \times 10^2$	$4.30 \times 10^{-2}$	$2.20 \times 10^{-1}$
5	$9.60 \times 10^{-3}$	$5.41 \times 10^{-3}$	$2.46 \times 10^{-4}$	$4.65 \times 10^{-5}$
6	$3.83 \times 10^{-3}$	$3.99 \times 10^{-3}$	$1.20 \times 10^{-3}$	$5.10 \times 10^{-4}$
7	$6.17 \times 10^{-2}$	$2.96 \times 10^2$	$3.67 \times 10^{-2}$	$5.19 \times 10^{-1}$
8	3.91	$4.38 \times 10^2$	$3.47 \times 10^{-2}$	$1.99 \times 10^{-2}$
9	$1.27 \times 10^{-2}$	$9.38 \times 10^{-3}$	$4.06 \times 10^{-4}$	$6.46 \times 10^{-4}$
10	$5.28 \times 10^{-1}$	$2.02 \times 10$	$4.37 \times 10^{-2}$	$1.36 \times 10^{-1}$
11	$9.66 \times 10^{-2}$	6.98	$5.21 \times 10^{-3}$	$5.04 \times 10^{-2}$
12	$7.33 \times 10^{-1}$	$4.95 \times 10$	$1.80 \times 10^{-2}$	$1.63 \times 10^{-1}$
13	$2.48 \times 10^{-1}$	$2.48 \times 10$	$1.32 \times 10^{-2}$	$2.12 \times 10^{-1}$
14	$2.68 \times 10^{-1}$	$2.35 \times 10$	$1.46 \times 10^{-2}$	$1.92 \times 10^{-1}$
15	$2.59 \times 10^{-1}$	$2.82 \times 10$	$1.45 \times 10^{-2}$	$2.40 \times 10^{-1}$

( $\epsilon$ -caprolactone) was caused by erosion, and thus we believe that our previous model could be sufficiently adapted to the case given in this paper. When adapting our empirical mathematical models, it is better to make adequate judgment about the physicochemical characteristics of the actual wax matrix dosage forms and to apply the model that reflects the physicochemical character more accurately.

#### 4.3. Results of parameter estimation and multi-regression analysis

**Table 5** lists values of the two diffusion coefficient parameters for the TDD model,  $K$  and  $k$ , obtained by fitting the TDD model (Eq. (13)) to the experimental data. **Table 6** shows the results of the multi-regression analysis. In this analysis, each  $K$  and  $k$  parameter was converted into logarithm for all parameters to show positive values when adapted to multi-regression analysis. Further, Figs. 4 and 5 display response surface plots for  $\log K$  and  $\log k$ , respectively, created by fixing each particle diameter within the different test batches.

Fig. 4(A) shows the plot to determine the effect of APAP loading ( $x_1$ ) and AMCE loading ( $x_2$ ) on  $\log K$  at pH 6.5, when particle diameter ( $x_3$ ) is fixed at -1, 0, or 1. As can be seen from this figure, an increase in  $\log K$  was observed as the AMCE loading ( $x_2$ ) increased; suggesting a rapid increase in the diffusion coefficient. This might be explained by the expansion of pores within the wax matrix particles due to the water solubility characteristics of AMCE. The logarithm of  $K$  was found to increase as  $x_3$  decreased. Previously, some researchers have reported that an increase in relative drug release rates coincides with a decrease in particle diameter of

cylindrical and spherical wax matrix dosage forms, owing to differences in the length of the diffusion pathways (Verhoeven et al., 2009; Cheboyina and Wyandt, 2008). Therefore, the present result could also be explained by the differences in the length of the diffusion pathways within the particles, and for the case of particles with a small particle diameter, this produced an increase in the relative APAP release rates. Fig. 4(B) shows the plot to determine the effect of  $x_1$  and  $x_2$  on the logarithm of  $K$  for different particle diameters at pH 4.0. An increase in AMCE loading ( $x_2$ ) was found to affect  $\log K$ . This might be explained by the fact that AMCE dissolves immediately below pH 5.0. These results indicate that the dissolution and diffusion of AMCE were involved in producing changes in the wax matrix pores.

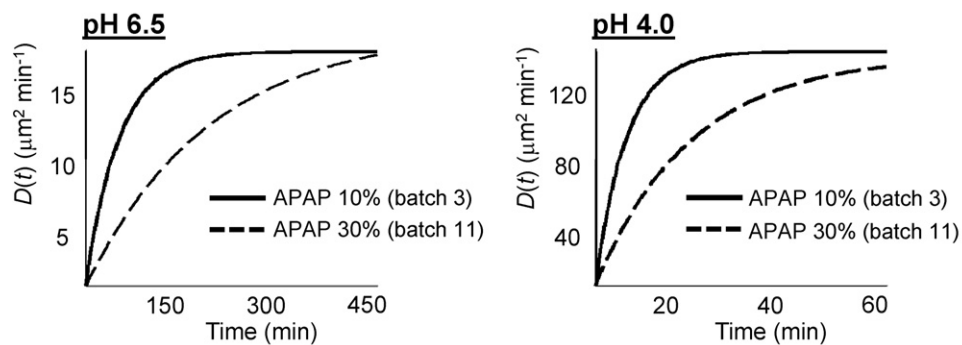
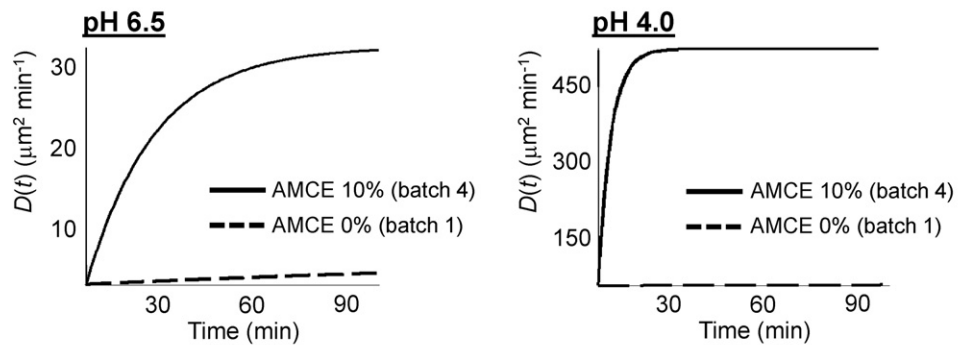
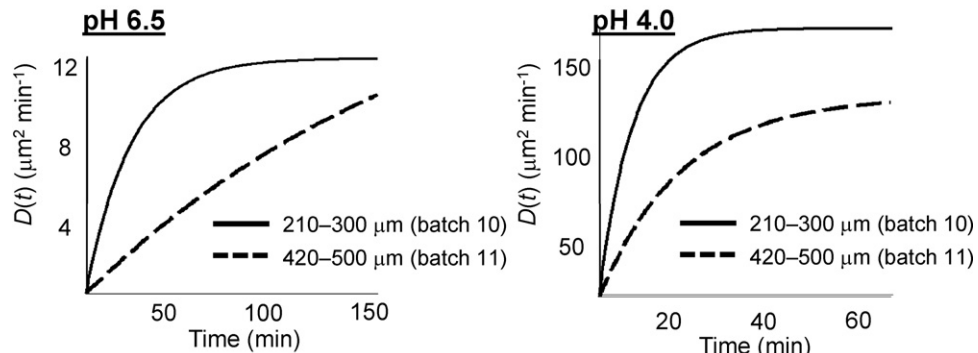
Fig. 5(A) shows the plot to determine the effect of  $x_1$  and  $x_2$ , for fixed  $x_3$ , on the logarithm of  $k$  at pH 6.5. An increase in logarithm of  $k$  was observed as the AMCE loading increased; that is, the diffusion coefficient rapidly reaches a maximum ( $K/k$ ). In addition,  $\log k$  increased with a decrease in value of  $x_3$ . This result also reflected that a phenomenon, such as a decrease in the length of the diffusion pathways, occurred. Fig. 5(B) shows a plot of changes in  $\log k$  at pH 4.0. Similarly, an increase in  $\log k$  was observed as the AMCE loading increased and was also attributable to the pH-dependent dissolution of AMCE. Furthermore, the reason that  $k$  depends weakly on  $x_1$  and  $x_3$ , relative to  $x_2$ , can also be explained by the above property of AMCE.  $K$  values are larger than  $k$  values for each formulation. Hence, in comparison to  $k$  values,  $K$  values are found to significantly affect the time-dependent change of the diffusion coefficient.

By means of the results of  $k$  and  $K$  values, the time-dependent changes of the diffusion coefficient  $D(t)$  were illustrated in Fig. 6. To determine the effect of the amounts of drug loading ( $x_1$ ), e.g., between batch 3 and 11 which contains 10% or 30% APAP for fixed with AMCE( $x_2$ ) loading and particle diameter( $x_3$ ), a decrease in  $D(t)$  was observed as  $x_1$  increased (Fig. 6(A)). Similarly, prepared batch that contained a high amount of drug tended to show slower drug release than one that contained a low amount of drug for almost all the batches (data not shown). Previously, Cheboyina and Wyandt (2008) reported that drug release kinetics changed depending on the difference in drug solubility and drug loading. Therefore, when the APAP loading was increased, the dissolution process, as well as diffusion process, would influence the release of APAP from the prepared wax matrix particles, and a much lower drug release rate would be observed. In addition, when determining the effects of AMCE loading ( $x_2$ ) and particle diameter ( $x_3$ ) on the changes of  $D(t)$ , an increase in  $D(t)$  was observed as  $x_2$  increased and  $x_3$  decreased (Fig. 6(B) and (C)). In particular, comparing with higher pH condition such as pH 6.5, higher  $D(t)$  values and faster speed which  $D(t)$  reaches a maximum were observed in lower pH condition (Fig. 6). These phenomena can be attributed to the pH-dependent

**Table 6**Multiple regression analysis of  $\log K$  and  $\log k$  at pH 6.5 and pH 4.0.

	pH 6.5		pH 4.0	
	$\log K$ ( $\mu\text{m}^2 \text{min}^{-2}$ )	$\log k$ ( $\text{min}^{-1}$ )	$\log K$ ( $\mu\text{m}^2 \text{min}^{-2}$ )	$\log k$ ( $\text{min}^{-1}$ )
$x_1$	$-1.6 \times 10^{-1}^*$	$-2.4 \times 10^{-1}^*$	$-1.8 \times 10^{-1}$	$-2.0 \times 10^{-1}$
$x_2$	$9.3 \times 10^{-1}^*$	$7.9 \times 10^{-1}^*$	$2.2^*$	$1.4^*$
$x_3$	$-3.2 \times 10^{-1}^*$	$-5.0 \times 10^{-1}^*$	$-1.3 \times 10^{-1}$	$-2.2 \times 10^{-1}^*$
$x_1^2$	$2.6 \times 10^{-1}^*$	$4.0 \times 10^{-1}^*$	$-1.3 \times 10^{-1}$	–
$x_2^2$	$-5.4 \times 10^{-1}^*$	$-7.8 \times 10^{-1}^*$	$-1.4^*$	$-1.3^*$
$x_3^2$	$-1.2 \times 10^{-1}^*$	$-2.2 \times 10^{-1}$	–	$-1.9 \times 10^{-1}$
$x_1 x_2$	–	–	–	–
$x_1 x_3$	$-8.3 \times 10^{-2}^*$	–	–	–
$x_2 x_3$	$-5.5 \times 10^{-1}^*$	$1.8 \times 10^{-1}$	–	$3.2 \times 10^{-1}^*$
Constant	$-6.0 \times 10^{-1}^*$	$-1.9^*$	$1.4^*$	$-6.4 \times 10^{-1}^*$

\*  $p < 0.05$ .

**A) AMCE 5%, fraction 420–500  $\mu$ m****B) APAP 10%, fraction 300–420  $\mu$ m****C) APAP 30%, AMCE 5%**

**Fig. 6.** Effect of (A) drug loading ( $x_1$ ), (B) AMCE loading ( $x_2$ ) and (C) particle diameter ( $x_3$ ) on the time-dependent changes of diffusion coefficient at pH 6.5 and pH 4.0.

dissolution of AMCE as mentioned above. Thus, a use of two parameters  $K$  and  $k$  obtained from TDD model could be sufficient to consider the effects of each factor in formulations against drug release behavior and figure out the time-dependent changes of diffusion coefficient.

#### 4.4. Prediction of drug release behavior

From the results of multi-regression analysis mentioned above, APAP loading, AMCE loading, and particle diameter affected the time-dependent change of diffusion coefficient. By applying the obtained results, a design for wax matrix particles with desirable drug release behavior would be possible. In the present study, as an example, we restricted the behavior to the following criteria taking the bitter taste masking of APAP without lowering the bioavailability into consideration: the amount of

APAP released from wax matrix particles with a diameter of 400  $\mu$ m must be below 15% for 10 min at pH 6.5, whereas at pH 4.0, 90% of the APAP must be released within 30 min. Fig. 7 shows the drug release ratio at 30 min in pH 4.0 buffer solution (red graduation) and the ratio at 10 min in pH 6.5 buffer solution (blue graduation). To meet the desired criteria of the drug release behavior, 15% APAP loading and 8.25% AMCE loading were chosen.

Based on the predicted loadings, wax matrix dosage forms were prepared, and drug release studies were conducted. In Fig. 8, the solid curve denotes the drug release profile at pH 4.0 and dashed curve denotes the drug release profile at pH 6.5. The predicted drug release behavior agreed well with the experimental values at each pH level, indicating that the TDD model can provide highly precise and valid predictions for wax matrix dosage forms.

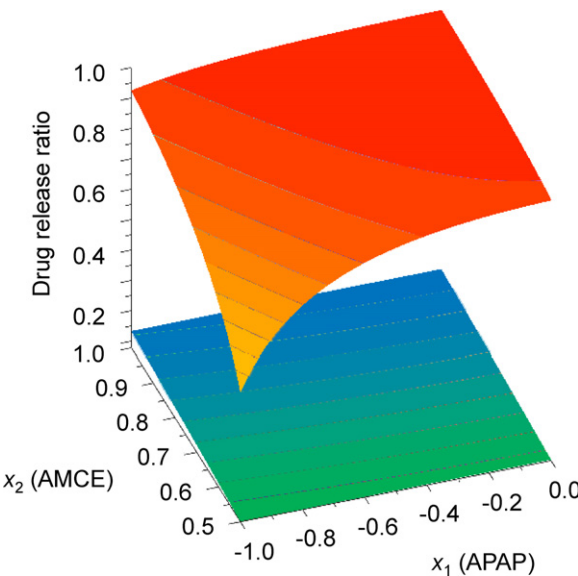


**Fig. 7.** Response surfaces. (red graduation) Drug release ratio at 30 min in pH 4.0 and (blue graduation) drug release ratio at 10 min in pH 6.5. (For interpretation of the references to color in this figure legend, the reader is referred to the web version of the article.)

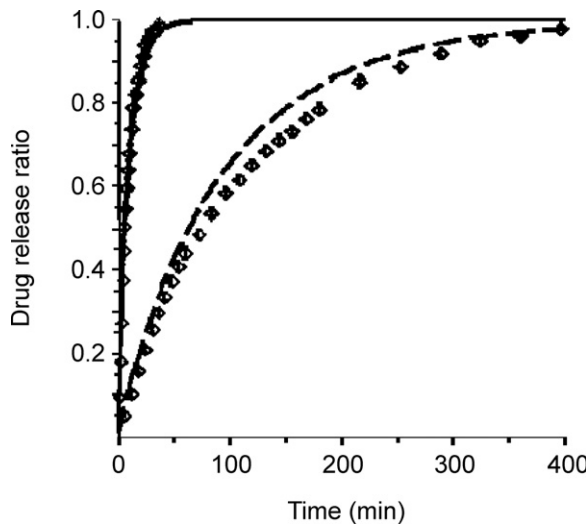


**Fig. 8.** Predicted drug release profiles and experimental values. Solid curve denotes drug release profile in pH 4.0 and dashed curve denotes drug release profile in pH 6.5. Symbols represent the mean  $\pm$  S.D. ( $n=3$ ).

## 5. Conclusions

In this study, based on the hypothesis that the structural changes of wax matrix particles are related to the time-dependent changes of the diffusion coefficient, we derived a new mathematical model (TDD model) and determined its validity. Since the TDD model agreed well with all experimental data, the TDD model is superior to the conventional pure diffusion model. In addition, by using a combination of the TDD model and a Box–Behnken design, the

influences of APAP loading, AMCE loading, and particle diameter on two parameters ( $K$  and  $k$ ) were revealed.  $K$  and  $k$  are associated with the time-dependent structural changes inside wax matrix dosage forms, and they provide insight into the drug release mechanism. Furthermore, when a wax matrix was prepared by using the TDD model in order to satisfy desired criteria, good agreement with the experimental values was observed. Accordingly, this TDD model is expected to be a useful tool for designing formulations of wax matrix dosage forms.

## Acknowledgment

The authors thank the Iwaki Seiyaku Co., Ltd. (Shizuoka, Japan) for kindly providing APAP for this study.

## References

- Agata, Y., Iwao, Y., Shiino, K., Miyagishima, A., Itai, S., 2011. A theoretical approach to evaluate the release rate of acetaminophen from erosive wax matrix dosage forms. *Int. J. Pharm.* 414, 63–68.
- Albertini, B., Passerini, N., Patarino, F., Rodriguez, L., 2008. New spray congealing atomizer for the microencapsulation of highly concentrated solid and liquid substances. *Eur. J. Pharm. Biopharm.* 69, 348–357.
- Anees, A.K., Mansoor, A.K., 1996. Box–Behnken design for the optimization of formulation variables of indomethacin coprecipitates with polymer mixtures. *Int. J. Pharm.* 131, 9–17.
- Cheboyina, S., Wyandt, C.M., 2008. Wax-based sustained release matrix pellets prepared by a novel freeze pelletization technique II. In vitro drug release studies and release mechanisms. *Int. J. Pharm.* 359, 167–173.
- Crank, J., 1975. *The Mathematics of Diffusion*. Clarendon Press, Oxford.
- Ferreira, S.L.C., Bruns, R.E., Ferreira, H.S., Matos, G.D., David, J.M., Brandão, G.C., da Silva, E.G.P., Portugal, L.A., dos Reis, P.S., Souza, A.S., dos Santos, W.N.L., 2007. Box–Behnken design: an alternative for the optimization of analytical methods. *Anal. Chim. Acta* 597, 179–186.
- Higuchi, T., 1961. Rate of release of medicaments from ointment bases containing drugs in suspension. *J. Pharm. Sci.* 50, 874–875.
- Kayumba, P.C., Huyghebaert, N., Cordella, C., Ntwakulirayo, J.D., Vervaet, C., Remon, J.P., 2007. Quinine sulphate pellets for flexible pediatric drug dosing: formulation development and evaluation of taste-masking efficiency using the electronic tongue. *Eur. J. Pharm. Biopharm.* 66, 460–465.
- Mönkkäri, J., Hakala, R.A., Vlasova, M.A., Huotari, A., Kilpeläinen, M., Kiviniemi, A., Meretoja, V., Herzig, K.H., Korhonen, H., Seppälä, J.V., Järvinen, K., 2010. Biocompatible photocrosslinked poly(ester anhydride) based on functionalized poly( $\epsilon$ -caprolactone) prepolymer shows surface erosion controlled drug release in vitro and in vivo. *J. Control. Release* 146, 349–355.
- Neau, S.H., Howard, M.A., Claudiu, J.S., Howard, D.R., 1999. The effect of the aqueous solubility of xanthine derivatives on the release mechanism from ethylcellulose matrix tablets. *Int. J. Pharm.* 179, 97–105.
- Raman, C., Berkland, C., Kim, K., Pack, D.W., 2005. Modeling small-molecule release from PLG microspheres: effects of polymer degradation and nonuniform drug distribution. *J. Control. Release* 103, 149–158.
- Shiino, K., Iwao, Y., Miyagishima, A., Itai, S., 2010. Optimization of a novel wax matrix system using aminoalkyl methacrylate copolymer E and ethylcellulose to suppress the bitter taste of acetaminophen. *Int. J. Pharm.* 395, 71–77.
- Siepmann, F., Herrmann, S., Winter, G., Siepmann, J., 2008. A novel mathematical model quantifying drug release from lipid implants. *J. Control. Release* 128, 233–240.
- Takayama, K., Okabe, H., Obata, Y., Nagai, T., 1990. Formulation design of indomethacin gel ointment containing *d*-limonene using computer optimization methodology. *Int. J. Pharm.* 61, 225–234.
- Verhoeven, E., Siepmann, F., De Beer, T.R.M., Van Loo, D., Van den Mooter, G., Remon, J.P., Siepmann, J., Vervaet, C., 2009. Modeling drug release from hot-melt extruded mini-matrices with constant and non-constant diffusivities. *Eur. J. Pharm. Biopharm.* 73, 292–301.
- Xu, J., Bovet, L.L., Zhao, K., 2008. Taste masking microspheres for orally disintegrating tablets. *Int. J. Pharm.* 359, 63–69.
- Yajima, T., Nogata, A., Demachi, M., Umeki, N., Itai, S., Yunoki, N., Nemoto, M., 1996. Particle design for taste-masking using a spray-congealing technique. *Chem. Pharm. Bull.* 44, 187–191.